



Noncyclic Diaza Ligands and Their Metal Complexes: Synthesis, Characterization and Biological Studies

PRANTA SARKER¹, AVIJIT CHAKRABORTY¹, SASWATA RABI², PRADIP PAUL¹, FONI BUSHON BISWAS¹,
KANAK BARUA¹, ISMAIL M. M. RAHMAN^{3,*} and TAPASHI GHOSH ROY^{1,*}

¹Department of Chemistry, Faculty of Science, University of Chittagong, Chattogram 4331, Bangladesh

²Department of Chemistry, Chittagong University of Engineering & Technology, Chattogram 4349, Bangladesh

³Institute of Environmental Radioactivity, Fukushima University, 1 Kanayagawa, Fukushima City, Fukushima 960-1296, Japan

*Corresponding authors: E-mail: immrahman@ipc.fukushima-u.ac.jp; tapashir57@cu.ac.bd

Received: 26 September 2023;

Accepted: 30 October 2023;

Published online: 2 December 2023;

AJC-21465

Condensation reactions involving various ketones and amines formed noncyclic ligands denoted as L^I, L^{II}, L^{III} and L^{IV}. Ethylenediamine, when reacted with acetophenone, benzoylacetone (in the presence of 70% HClO₄) and benzophenone, resulted in the following noncyclic ligands: (*E,E*)-*N,N*-bis(1-phenylethylidene)ethylenediamine (L^I), *bis*(1-3-hydroxy-3-phenylbut-2-ene-ylidene) (L^{II}) and (*E,E*)-*N,N*-bis(1,1-diphenylmethylidene)ethylenediamine (L^{III}), respectively. The reaction of benzophenone with 1,3-diaminopropane in a 1:1 ratio in a methanolic solution also led to the synthesis of a noncyclic ligand, (*E,E*)-*N,N*-bis(1,1-diphenylmethylidene)propylenediamine (L^{IV}). All the synthesized noncyclic ligands, except L^{II}, undergo decomposition during complexation, reverting to the initial ketones and amines. In contrast, L^{II} exhibits remarkable stability and can form square planar complexes with Ni(II), Cu(II), and Co(II) salts. Additionally, the Co(II) complex can convert into a six-coordinated Co(III) complex, [CoL^{II}(H₂O)₂](NCS), when it reacts with KNCS. All these ligands and derived metal complexes were characterized and their antimicrobial properties were evaluated against the selected fungi and bacteria.

Keywords: Noncyclic ligands, Metal complexes, Spectroscopic studies, Antimicrobial activities.

INTRODUCTION

The field of coordination chemistry continually motivates us to create novel ligands and investigate their compatibility and complex-forming abilities with various metal ions. As per previous studies, several macrocyclic ligands and their derivatives have been successfully synthesized using different ketones and amines [1-5]. Continuing the research, designing new macrocycles has been attempted by altering the initial ketones (acetophenone, benzoylacetone or benzophenone) and amines (ethylenediamine or 1,3-diaminopropane). However, these efforts did not yield the desired macrocycles instead, they led to the formation of the following noncyclic ligands: (*E,E*)-*N,N*-bis(1-phenylethylidene)ethylenediamine (L^I), *bis*(1-3-hydroxy-3-phenylbut-2-ene-ylidene) (L^{II}), (*E,E*)-*N,N*-bis(1,1-diphenylmethylidene)ethylenediamine (L^{III}) and (*E,E*)-*N,N*-bis(1,1-diphenylmethylidene)propylenediamine (L^{IV}) (Fig. 1). This unexpected outcome prompted whether these noncyclic

ligands can form complexes with different metal salts. Investigations showed that L^I, L^{III} and L^{IV} decompose during complexation, resulting in the formation of complexes with the initial amines, which was confirmed through analytical and various spectroscopic analyses. On the contrary, L^{II} formed four-coordinated square planar complexes with Ni(II), Cu(II) and Co(II) when reacted with the respective metal salts. Furthermore, Co(II) complex, [CoL^{II}], transformed into a six-coordinated Co(III) complex, [CoL^{II}(H₂O)₂](NCS), upon interaction with KNCS.

Previous studies showed that Cu(II), Ni(II), Co(II) and Co(III) complexes derived from macrocyclic ligands with analogous starting materials possess potent antimicrobial properties [1-6]. Therefore, the antimicrobial effectiveness of the noncyclic ligands and the newly synthesized Cu(II), Ni(II), Co(II), and Co(III) complexes of L^{II} have been investigated. In this work, the synthesis, characterization, antibacterial and antifungal activities of the noncyclic ligands (L^I, L^{II}, L^{III} and L^{IV}) as well

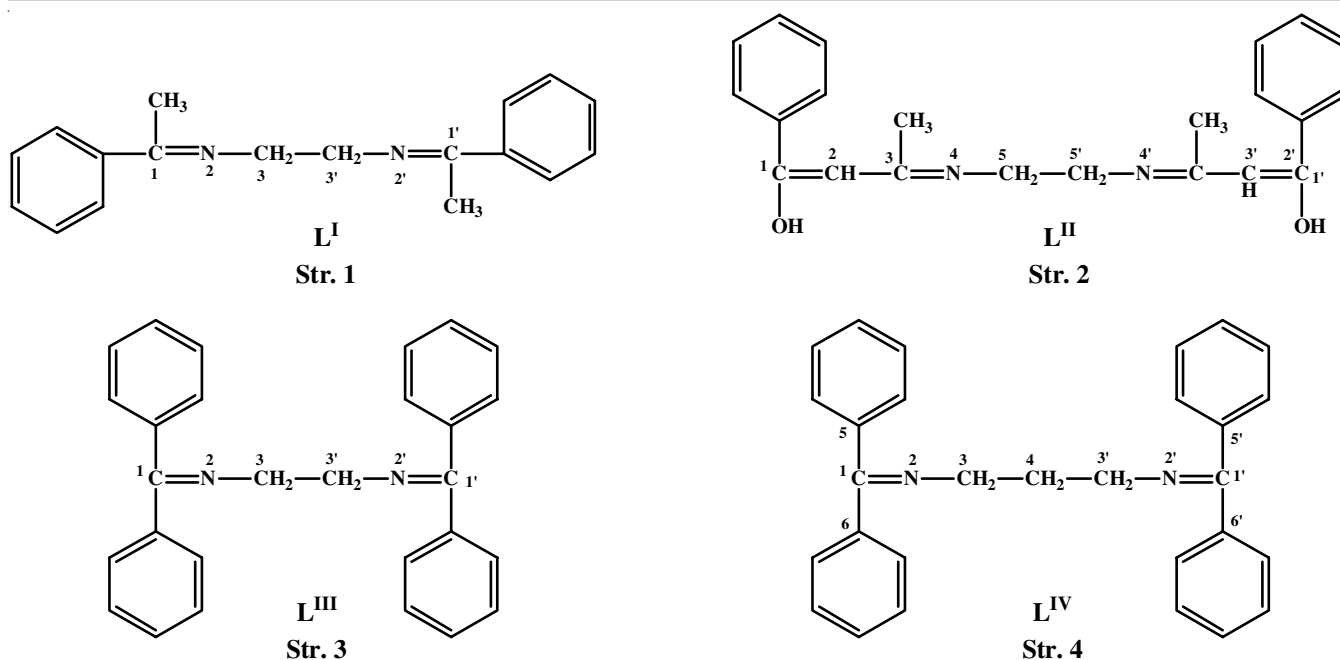


Fig. 1. Structures of the noncyclic ligands

as Cu(II), Ni(II), Co(II) and Co(III) complexes of L^I, have been reported.

EXPERIMENTAL

Analytical-grade chemicals obtained from Sigma Aldrich (St. Louis, USA) were used without additional purification. Reagent-grade solvents were used after drying by following standard procedures. Standard laboratory equipments were utilized for the experiments.

Synthesis of ligands

Ligand L^I: In a 250 mL conical flask, 0.1 mmol (6.7 mL) of 1,2-diaminoethane was mixed with 30 mL of acetophenone. The solution was stirred using a magnetic stirrer for 3 h while maintaining a temperature at the range of 70-80 °C. As the reaction progressed, the colour of the mixture changed to brown. Subsequently, the reaction mixture was left undisturbed at room temperature overnight, during which crystals formed. These crystals were separated by filtration, subjected to 3-4 times ethanol washes until the brown color completely vanished, and finally rinsed with ether. The resulting product underwent recrystallization in xylene, resulting in a white crystalline substance that was subsequently dried under a vacuum. Further concentration of the residual solution provided another batch of the product, which exhibited an infrared spectrum identical to that of the initial crop. The overall yield of the process was approximately 75%. Colour: white, *m.w.*: 264.36. Anal. calcd. (found) %: C, 80.84 (80.80); H, 8.68 (8.57); N, 10.48 (10.57). IR (KBr, ν_{\max} , cm^{-1}): 2920 (C-H); 3020 (Ar-H); 1394 (CH₃), 1610 (C=N), 1083 (C-C), 756, 687 (C-H) Ar. Mass (*m/z*): M⁺ peak, 264; Base peak, 91; fragment peak, 146, 132, 130, 104, 103, 41. ¹H NMR (δ , ppm in DMSO-*d*₆): (for CH₃), 2.25 (s, 3H), 2.50 (s, 3H); (for CH₂), 2.27(t, 4H); (for phenyl), 7.35 (m, 5H), 7.85 (m, 5H). ¹³C NMR (δ , ppm in DMSO-*d*₆), Methyl

carbons, 14.4; CH₂ carbon, 51.8; phenyl carbons, 126.5, 126.8, 127.5, 139.7; *sp*² carbons, 164.6.

Ligand L^{II}: Benzoylacetone (0.02 mmol, 0.324 g) was suspended in 50 mL methanol. To this suspension, 1.32 mL (0.02 mmol) of 1,2-diaminoethane was added, resulting in a clear solution. While stirring on a magnetic stirrer, 1.98 mL (0.02 mmol) of 70% HClO₄ was slowly added from a dropping funnel. The reaction temperature was maintained at 60-65 °C, and a light brown color developed at this stage. After 1 h, the white product began to precipitate. The reaction mixture was stirred for an additional 2 h, followed by allowing it to stand undisturbed at room temperature overnight. The resulting white solid product was separated by filtration, washed sequentially with methanol, ethanol and finally with ether. Subsequently, the white product was dried under a vacuum. Concentrating the remaining solution produced an additional batch of the product, which exhibited an infrared spectrum identical to that of the initial batch. The overall yield of this process was approximately 60%. The same product can be synthesized without HClO₄ under identical conditions. However, it was observed that in the absence of HClO₄, the reaction proceeded at a slower rate, resulting in a comparatively lower yield and longer reaction time. The yield obtained without HClO₄ was about 35%. Colour: white. *m.w.*: 348.44. Anal. calcd. (found) %: C, 75.86 (75.80); H, 6.89 (6.82); N, 8.04 (8.11). IR (KBr, ν_{\max} , cm^{-1}): 2920 (C-H); 3030 (Ar-H); 1380 (CH₃); 1603 (C=N); 1065 (C-C); 3400 (O-H); 711, 692 (C-H)Ar. ¹H NMR (δ , ppm in DMSO-*d*₆): (for CH₃), 2.04 (s, 6H); (for CH₂), 3.53 (t, 4H); (for phenyl), 7.39 (m, 5H), 7.85 (m, 5H); (for CH and OH), 5.68 (s, 2H), 11.54 (2H). ¹³C NMR (δ , ppm in DMSO-*d*₆): Methyl carbons, 19.2; CH₂ carbon, 43.7; *sp*² CH carbon, 92.9; phenyl carbons, 126.9, 128.1, 130.6, 140.1; *sp*² C carbons, 164.8, 188.2.

Ligand L^{III}: Benzophenone (0.1 mmol, 1.82 g) dissolved in 50 mL of dry methanol was added to 3.35 mL (0.1 mmol)

of 1,2-diaminoethane. This solution was stirred using a magnetic stirrer for 3 h, maintaining the temperature between 70-80 °C. Following this heating step, the reaction mixture was left at room temperature for 24 h and separated into two distinct layers. There were two distinct layers, one aqueous and the other was viscous. The viscous layer was isolated using a separating funnel and left at room temperature. As the solvent evaporated, a white solid product formed. This product was filtered, washed with methanol several times, and recrystallized from a 3:1 ethanol-chloroform mixture. Finally, it was washed with ether and the resulting white crystalline product was dried over silica gel under vacuum. The overall yield was approximately 68%. Colour: white, *m.w.*, 388.50. Anal. calcd. (found) %: C, 86.59 (86.50); H, 6.18 (6.05); N, 7.21 (7.11). IR (KBr, ν_{\max} , cm^{-1}): 2915 (C–H); 3030 Ar–H (C–H), 1396 (CH_3); 1603 (C=N); 1074 (C–C); 711 (C–H)Ar. Mass (*m/z*): M^+ peak, 388; Base peak, 194; fragment peak, 208, 180, 166, 103. $^1\text{H NMR}$ (δ , ppm in DMSO- d_6): for CH_2 , 7.20 (m, 4H); for phenyl, 7.28 (m, 5H), 7.40 (m, 5H), 7.51 (m, 5H), 7.65 (m, 5H). $^{13}\text{C NMR}$ (δ , ppm in DMSO- d_6), CH_2 carbon, 55.2; phenyl carbons, 127.0, 128.0, 128.3, 128.4, 129.8, 136.9, 139.9; sp^2 carbons, 168.8.

Ligand L^{IV}: Benzophenone (0.2 mmol, 3.64 g) was combined with 40 mL of methanol in a 250 mL conical flask and 1.68 mL (0.2 mmol) of 1,3-diaminopropane was added to the mixture. The reaction mixture was subjected to reflux with stirring on a magnetic stirrer for 3 h, maintaining the temperature between 70-80 °C. The reaction mixture remained undisturbed at room temperature overnight after the heating phase. The resulting solid product was separated by filtration, washed with ethanol multiple times and rinsed with ether. The fine white product obtained was subsequently dried under a vacuum. Concentration of the remaining solution provided an additional batch of the product, which exhibited an infrared spectrum identical to that of the initial batch. The overall yield of this process was approximately 65%. Colour: white, *m.w.* 402.53. Anal. calcd. (found) %: C, 86.56 (86.48); H, 6.46 (6.40); N, 6.96 (6.88); IR (KBr, ν_{\max} , cm^{-1}): 2932 (C–H); 3055 (Ar–H); 1595 (C=N), 1075 (C–C), 703, 696 (C–H)Ar. Mass (*m/z*): M^+ peak, 402; Base peak, 105; fragment peak, 222, 208, 194, 166, 131, 117, 77, 40. $^1\text{H NMR}$ (δ , ppm in DMSO- d_6): (for CH_2), 7.46 (m, 6H); (for phenyl), 7.57 (m, 10H), 7.80 (m, 10H). $^{13}\text{C NMR}$ (δ , ppm in DMSO- d_6), CH_2 carbon, 32.7, 51.7; phenyl carbons, 128.4, 129.9, 132.3, 137.8; sp^2 carbons, 196.5.

Synthesis of metal complexes of L^{II}: Ligand L^{II} in its noncyclic form (1.0 mmol, 0.348 g) was dissolved separately in 25 mL of hot methanol, along with 1.0 mmol of each of $\text{Ni}(\text{OCOCH}_3)_2 \cdot 4\text{H}_2\text{O}$, $\text{Cu}(\text{ClO}_4)_2 \cdot 6\text{H}_2\text{O}$ and $\text{Co}(\text{CH}_3\text{COO})_2 \cdot 4\text{H}_2\text{O}$. The resulting mixtures led to the formation of deep brown $[\text{NiL}^{\text{II}}]$, chocolate-coloured $[\text{CuL}^{\text{II}}]$, and orange-red $[\text{CoL}^{\text{II}}]$ compounds. To ensure completion of the reaction, the reaction mixtures were heated over a water bath for 25 min and then allowed to cool. Once cooled to room temperature, the colored products were filtered, washed with methanol followed by diethyl ether, and subsequently dried in a desiccator containing silica gel. The yield obtained ranged from approximately 67 to 73%. $[\text{NiL}^{\text{II}}]$ was also synthesized using NiCl_2 , $\text{Ni}(\text{NO}_3)_2$, NiSO_4 and $\text{Ni}(\text{ClO}_4)_2$. Similarly, $[\text{CuL}^{\text{II}}]$ and $[\text{CoL}^{\text{II}}]$ were

obtained using their respective chloride, nitrate, sulfate, perchlorate and acetate salts.

$[\text{NiL}^{\text{II}}]$: Colour: deep brown; *m.w.* 407.13. Anal. calcd. (found) %: C, 64.91 (64.87); H, 5.90 (5.97); N, 6.88 (6.75); Ni, 14.43 (14.35). IR (KBr, ν_{\max} , cm^{-1}): 2945 (C–H); 3024 (Ar–H); 1359 (CH_3), 1593 (C=N), 1074 (C–C); 696 (C–H)Ar; 559 (Ni–N). $^1\text{H NMR}$ (δ , ppm in DMSO- d_6): (for CH_3), 1.54 (s, 6H), 2.00 (s, a, 6H), (for CH_2), 3.13 (2H), 3.48 (2H), (for phenyl protons), 7.32 (m, 5H), 7.76 (m, 5H), (for CH), 5.64 (s, 2H). $^{13}\text{C NMR}$ (δ , ppm in DMSO- d_6), CH_3 carbons, 21.7; CH_2 carbon, 53.4; sp^2 CH carbon, 97.4; phenyl carbons, 126.6, 127.9, 129.3, 137.6; sp^2 carbons, 165.4, 171.5. Molar conductivity ($\text{ohm}^{-1} \text{cm}^2 \text{mol}^{-1}$), 0 (in DMSO), 0 (in CHCl_3). Magnetic moment (μ_{eff} , B.M.): diamagnetic. UV-vis [λ_{\max} in nm (ϵ_{\max})]: 731(42), 563(281), and 410(3913) (in DMSO).

$[\text{CuL}^{\text{II}}]$: Colour: chocolate, *m.w.* 411.99. Anal. calcd. (found) %: C, 64.14 (64.17); H, 5.83 (5.92); N, 6.80 (6.73); Cu, 15.43 (15.21). IR (KBr, ν_{\max} , cm^{-1}): 2933 (C–H); 3033 (Ar–H); 1355 (CH_3), 1595 (C=N); 1072 (C–C); 700 (C–H)Ar; 538 (Cu–N). Molar conductivity ($\text{ohm}^{-1} \text{cm}^2 \text{mol}^{-1}$): 0 (in DMSO), 0 (in CHCl_3). Magnetic moment (μ_{eff} , B.M.): 1.79. UV-vis [λ_{\max} in nm (ϵ_{\max})]: 549 (545) and 408 (3612) (in DMSO).

$[\text{CoL}^{\text{II}}]$: Colour: orange-red, *m.w.* 407.37. Anal. calcd. (found) %: C, 64.87 (64.87); H, 5.89 (5.97); N, 6.88 (6.72); Co, 15.48 (15.29). IR (KBr, ν_{\max} , cm^{-1}): 2939 (C–H), 3.29 (Ar–H); 1357 (CH_3); 1074 (C–C); 694 (C–H)Ar; 559 (Co–N). Molar conductivity ($\text{ohm}^{-1} \text{cm}^2 \text{mol}^{-1}$): 0 (in DMSO), 0 (in CHCl_3). Magnetic moment (μ_{eff} , B.M.): 1.75. UV-vis [λ_{\max} in nm (ϵ_{\max})]: 721(39), 480 and 356 (in DMSO); 548(545) and 404(3612) (in CHCl_3).

$[\text{CoL}^{\text{II}}(\text{H}_2\text{O})_2](\text{SCN})$: A solution of $[\text{CoL}^{\text{II}}]$ (0.406 g, 1.0 mmol) in 10 mL of chloroform was prepared and separately, 0.194 g (2.0 mmol) of KSCN was dissolved in 30 mL of methanol. The $[\text{CoL}^{\text{II}}]$ solution was added drop by drop into the KSCN solution with continuous stirring. The reaction mixture was heated on a water bath for 30 min, while the colour of the solution changed from orange-red to black. Subsequently, the reaction mixture was allowed to cool. Once it reached room temperature, black product was separated by filtration, washed with methanol followed by diethyl ether, and then dried in a desiccator containing silica gel. The yield obtained was approximately 32%.

$[\text{CoL}^{\text{II}}(\text{H}_2\text{O})_2](\text{NCS})$: Colour: black; *m.w.* 407.13. Anal. calcd. (found) %: C, 59.61 (59.51); H, 4.75 (4.81); N, 9.07 (8.96). IR (KBr, ν_{\max} , cm^{-1}): 3433 (–OH); 3033 (Ar–H); 2923 (C–H); 1384 (CH_3); 1070, 1026 (C–C), 705 (C–H)Ar, 555 (Co–N); 2047, 754, 476 (SCN); Molar conductivity ($\text{ohm}^{-1} \text{cm}^2 \text{mol}^{-1}$): 60 (in DMSO). Magnetic moment (μ_{eff} , B.M.): Diamagnetic. UV-vis [λ_{\max} in nm (ϵ_{\max})]: 707(39), 263(1785) and 261(1766) (in DMSO).

Physical measurements: Elemental analyses (C, H, N) were conducted using a Leco CHNS932 elemental analyzer from LECO Corporation (St. Joseph, MI, USA). NMR experiments (^1H , ^{13}C) were performed using a Bruker AVANCE 400 spectrometer from Bruker AG (Karlsruhe, Germany). Electrospray ionization (ESI) mass spectra were acquired using a MAT 95XL Finnigan instrument from ThermoQuest Finnigan (Bremen,

Germany). The UV-visible spectra were recorded in different solvents with a Shimadzu UV-visible spectrophotometer from Shimadzu (Kyoto, Japan). Conductance measurements were taken in DMSO and CH₃Cl using a HI-8820 conductivity bridge from Hanna Instruments (Padova, Italy). Magnetic moments were measured with a Gouy balance calibrated using Hg[Co(NCS)₄]. Infrared (IR) spectra were recorded in KBr discs using a Shimadzu IR 20 spectrophotometer from Shimadzu (Kyoto, Japan).

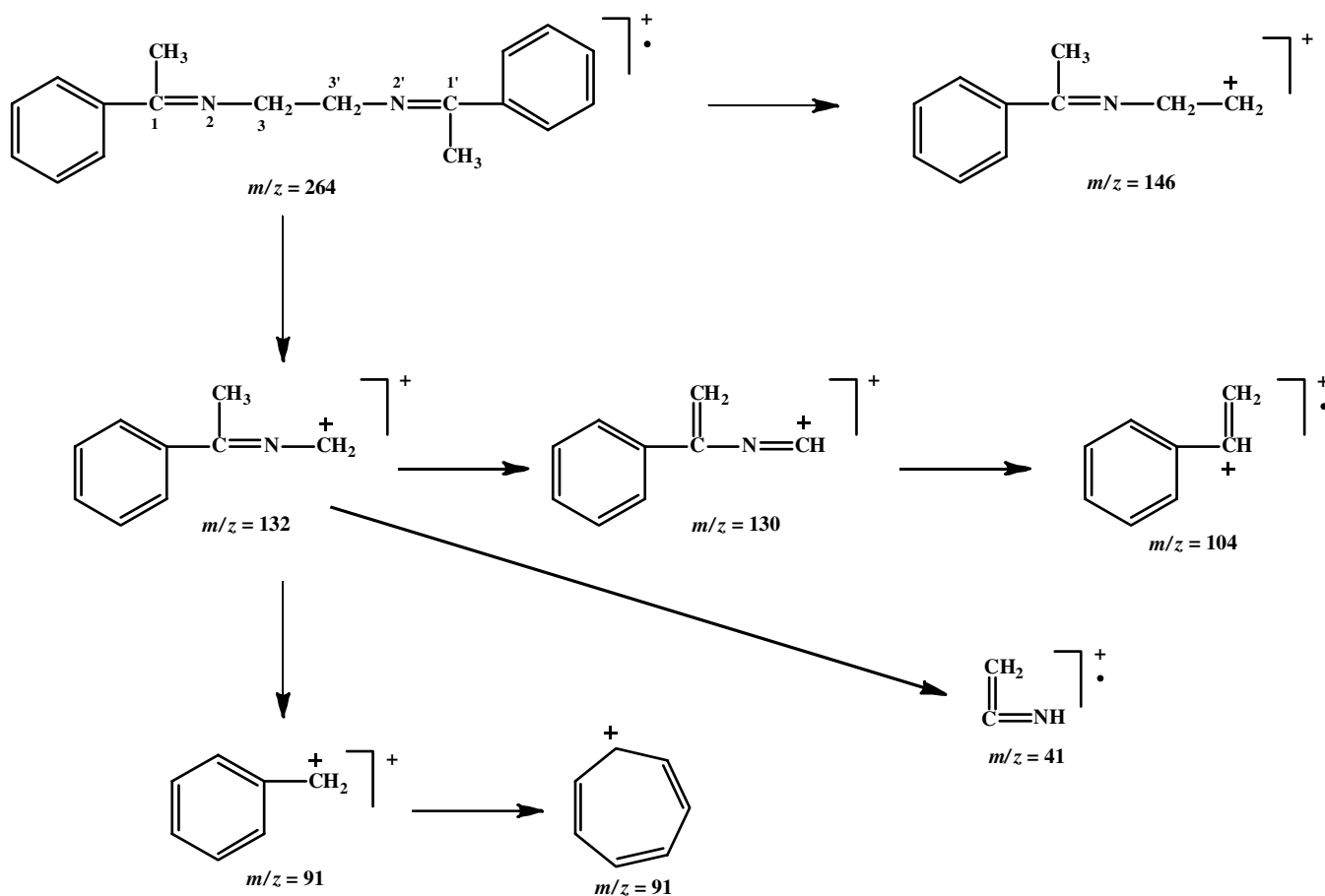
Antimicrobial efficacy: The antibacterial effectiveness of both the noncyclic ligands and the complexes of L^{II} was evaluated against four selected Gram-positive and six Gram-negative bacteria, utilizing the established methodology outlined in the literature [1-6]. Additionally, the antifungal properties of all the compounds were assessed, employing the approach previously described elsewhere [4].

RESULTS AND DISCUSSION

All the ligands, L^I, L^{II}, L^{III} and L^{IV} showed the presence of $\nu(\text{C-H})$, $\nu(\text{Ar-H})$, $\nu(\text{CH}_3)$, $\nu(\text{C=N})$, $\nu(\text{C-C})$ and $\nu(\text{C-H})\text{Ar}$ bands at 2932-2915, 3055-3020, 1396-1380, 1610-1595, 1083-1065 and 756-687, respectively, in their IR spectra. Moreover, prominent bands have appeared for mono-substituted benzene rings [7], which support the assigned ligand structure of L^I, L^{II}, L^{III} and L^{IV}.

For ligand L^I, the reaction of ethylenediamine with acetophenone yield the noncyclic ligand L^I, (*E,E*)-*N,N*-bis(1-phenylethylidene)ethylenediamine. The mass spectrum of this ligand (**Scheme-I**) displayed a peak at m/z 264, corresponding to the molecular ion [C₁₈H₂₀N₂]⁺. The base peak in the spectrum occurred at m/z 91. Typically, when an alkyl group substitutes an aromatic ring, a prominent peak is observed at m/z 91, attributed to the tropyllium ion (C₇H₇⁺) [8]. In this case, a benzyl cation (C₆H₅CH₂⁺) is formed and subsequently rearranges into the more stable tropyllium cation (C₇H₇⁺). The m/z 146 fragment is generated through the breaking of the C3'-N2' bond, while the m/z 132 fragment arises from the cleavage of the C3-C3' bond, resulting in a m/z 130 fragment after the removal of an H₂ molecule. This m/z 130 fragment subsequently produces a fragment at m/z 104 due to the cleavage of the C1-N2 bond. The m/z 132 fragment further undergoes fragmentation by breaking the Ar-C1 and N2-C3 bonds, forming a fragment at m/z 41.

The ¹H NMR spectrum exhibits a multiplet at 2.2 ppm and a singlet at 2.5 ppm. The multiplet at 2.2 ppm, corresponding to 7H, can be resolved into a singlet for one methyl group (3H) at 2.25 ppm and a triplet for two equivalent -CH₂-protons [(2+2)H] at 2.27 ppm. The singlet at 2.50 ppm, representing 3H, can be attributed to an additional methyl group located *trans*- to the other one. The presence of two multiplets at 7.35 and 7.85 ppm is likely due to two phenyl groups posit-



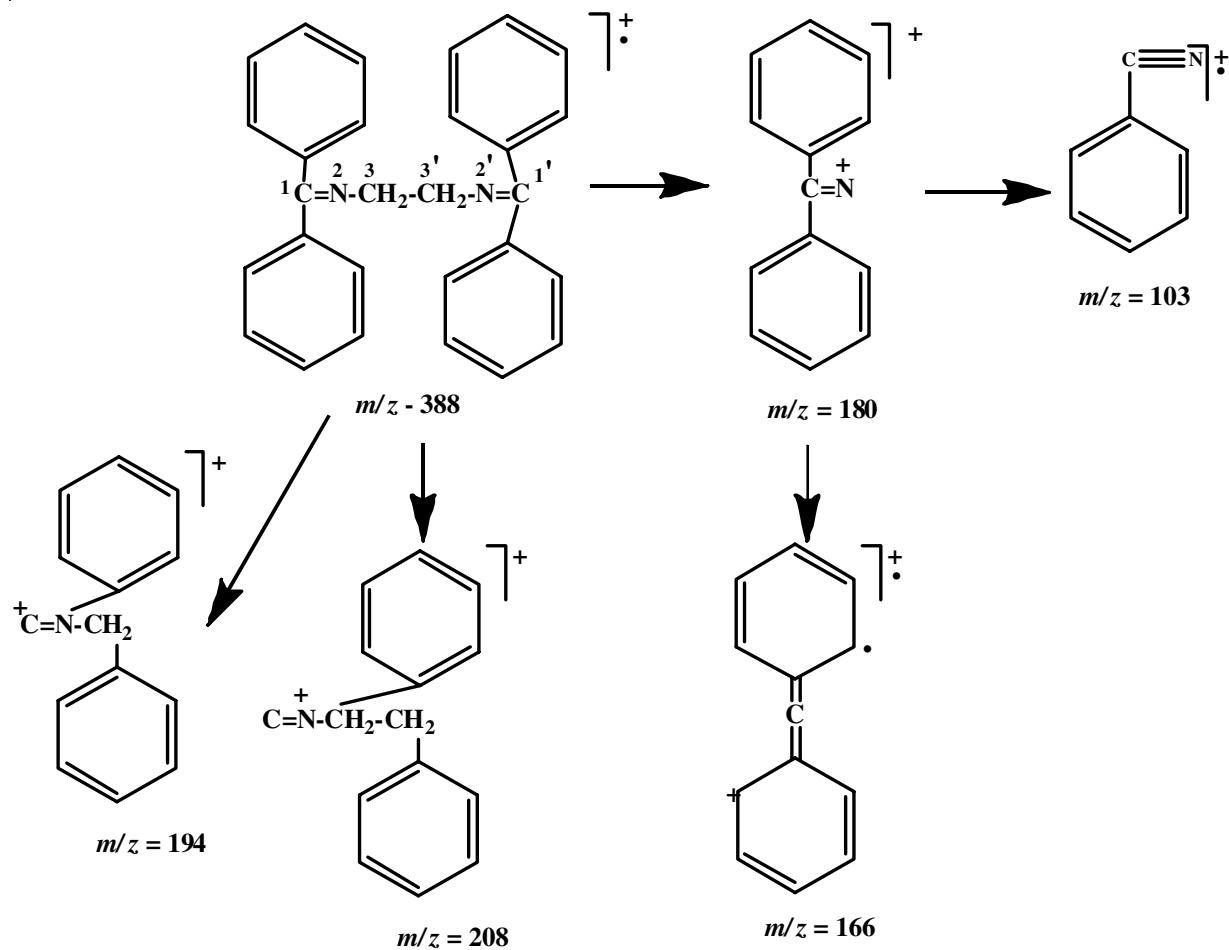
Scheme-I: Mass spectral fragmentation of the ligand L^I

ionized trans to each other. In ^{13}C NMR spectrum of this ligand, peaks appear at 14.4, 51.8, 126.5, 126.8, 127.5, 139.7 and 164.6 ppm. The peak at 14.4 ppm can be assigned to the carbons of two methyl groups, while the one at 51.8 ppm corresponds to the two carbons of two equivalent CH_2 groups. Typically, a mono-substituted benzene ring exhibits two equivalent carbons at *ortho*-positions, two equivalent carbons at two *meta*-positions, one carbon at the *para*-position, and another at the substituted position. Therefore, a mono-substituted benzene ring is expected to yield four signals and the two carbons attached to the phenyl group are anticipated to give a peak in the downfield region. Thus, the five peaks ranging from 126 to 165 ppm can be attributed to the carbons of two phenyl groups and the two other defined carbons.

For ligand L^{II} , the interaction of ethylenediamine with benzoylacetone in the presence of 70% HClO_4 resulted in the formation of a noncyclic ligand L^{II} , *bis*(1,3-hydroxy-3-phenylbut-2-ene-ylidene). The presence of the νOH band in its IR spectrum indicates that the ligand exists in its enol form. The ^1H NMR spectrum of this ligand reveals the presence of three singlets at 2.04, 5.68 and 11.54 ppm. The singlet at 2.04 ppm, representing 6H, corresponds to two CH_3 protons. The singlet at 5.68 ppm corresponds to two $-\text{CH}-$ protons and the most downfield singlet at 11.54 ppm (2H) corresponds to two $-\text{OH}$ protons. Additionally, the spectrum exhibits a triplet at 3.53

ppm, representing 4H, which can be attributed to the $-\text{CH}_2-\text{CH}_2-$ protons. Furthermore, two multiplets at 7.39 and 7.85 ppm, each corresponding to 5H, can be attributed to two sets of phenyl protons. The ^{13}C NMR spectrum of ligand L^{II} reveals the presence of 9 non-equivalent carbon atoms, and it displays 9 distinct signals. The signal at 19.2 ppm can be attributed to the equivalent methyl carbons on C(3) and C(3'), while the following two signals at 43.7 and 92.9 ppm correspond to two equivalent CH_2 (5, 5') carbons and two equivalent sp^2 carbons (2, 2') in CH groups, respectively. The most downfield signals at 188.2 and 164.8 ppm are associated with two equivalent sp^2 carbons (1, 1') attached to OH groups and two equivalent sp^2 carbons (3, 3') attached to N atoms, respectively. The remaining four signals at 126.9, 128.1, 130.6, and 140.1 ppm can be attributed to the 4 non-equivalent carbons in each of the two equivalent mono-substituted benzene rings.

For noncyclic ligand L^{III} , (*E,E*)-*N,N*-bis(1,1-diphenylmethylidene)ethylenediamine was obtained through the reaction of ethylenediamine with benzophenone. The mass spectrum (**Scheme-II**) reveals a peak at m/z 388, corresponding to the molecular ion $[\text{C}_{28}\text{H}_{24}\text{N}_2]^+$. The base peak is observed at m/z 194, resulting from the cleavage of C3-C3' bond. Additional fragments at m/z 208 and 180 are generated through the break-up of the $\text{N}2'-\text{C}3'$ bond. Further fragmentation of the fragment at m/z 180 yields fragments at m/z 166 and 103.

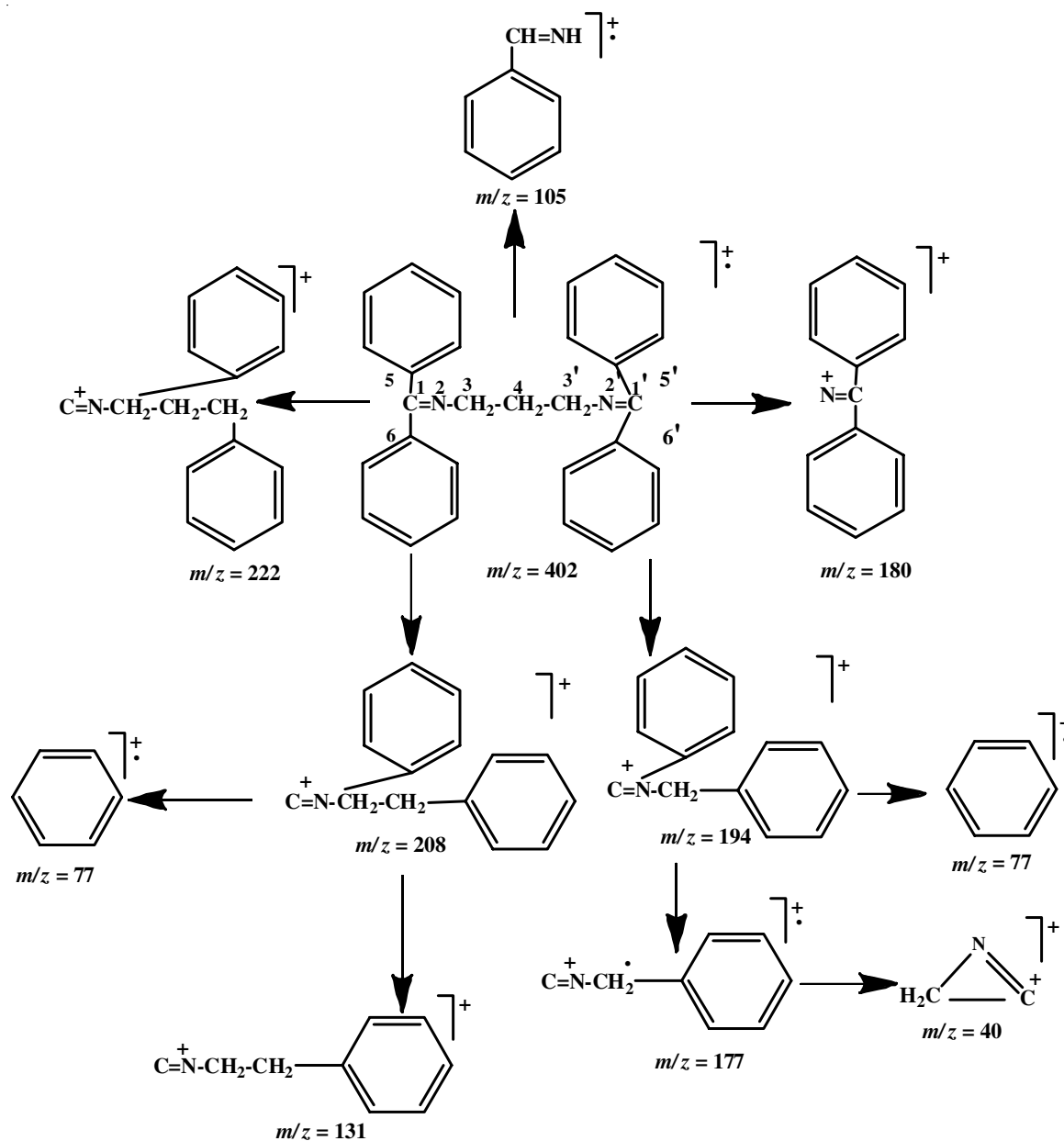


Scheme-II: Mass spectral fragmentation of ligand L^{III}

The ^1H NMR spectrum of this compound (L^{III}) is somewhat indistinct. However, due to the presence of four phenyl groups, all protons are likely deshielded. As a result, only five multiplets are observed in the region of 7.20 to 7.60 ppm. Among them, one at 7.20 ppm can be attributed to two CH_2 protons, while the other four at 7.28, 7.40, 7.51, and 7.65 ppm can be assigned to the four phenyl groups. The ^{13}C NMR spectrum of ligand L^{III} indicates the presence of two equivalent carbons in two CH_2 groups, two equivalent carbons in two sp^2 ($>\text{C}=\text{N}$) carbons, four non-equivalent carbons in each of two *trans-cis* oriented phenyl groups, and four non-equivalent carbons in each of the other two *trans-cis* oriented phenyl groups. Consequently, the ligand comprises a total of ten non-equivalent carbons. The ^{13}C NMR spectrum also exhibits 10 distinct peaks. The peak at 55.2 ppm can be attributed to two equivalent carbons in two CH_2 -groups, while the peak at 168.7 ppm corresponds

to two equivalent sp^2 ($>\text{C}=\text{N}$) carbons. The remaining eight peaks, falling within the range of 127 to 140 ppm, can be ascribed to four non-equivalent carbons in each of the two *trans-cis* oriented phenyl groups and the other four non-equivalent carbons in each of the other two *trans-cis* oriented phenyl groups.

For ligand L^{IV} , the reaction of benzophenone with 1,3-diaminopropane in a 1:1 ratio in a methanolic solution resulted in the formation of the noncyclic ligand L^{IV} , (*E,E*)-*N,N*-bis(1,1-diphenylmethylidene)propylenediamine. The mass spectrum of this ligand (**Scheme-III**) exhibits a peak at m/z 402, which correspond to the molecular ion $[\text{C}_{29}\text{H}_{26}\text{N}_2]^+$. Fragmentation of the molecular ion leads to a base peak at m/z 105, resulting from the cleavage of the $\text{N}-\text{CH}_2$ bond, as well as the removal of a phenyl group and the subsequent combination of two hydrogen atoms with $(\text{C}_6\text{H}_5)\text{C}=\text{N}$, forming the $(\text{C}_6\text{H}_5)\text{CH}=\text{NH}^+$ ion. The molecular ion experiences homolytic fission, primarily



Scheme-III: Mass spectral fragmentation of ligand L^{IV}

through the cleavage of the C4-C3' bond, yielding two fragments at m/z 208 and 194. Alternatively, the molecular ion also undergoes homolytic fission at the N2-C3 bond, resulting in two fragments at m/z 180 and 222. The fragment at m/z 194 further undergoes fragmentation at C1'-C5' or C1'-C6', leading to two fragments at m/z 117 and 77. The one at m/z 117 further yields a fragment at m/z 40 by the removal of the C₆H₅ group. On the other hand, the fragment at m/z 208 can also undergo fragmentation at C1-C5 or C1-C6, giving rise to two fragments at m/z 131 and 77.

The ¹H NMR spectrum of this ligand reveals signals within the range of 7.3 to 8.0 ppm. Three multiplets appearing in this region are observed in the ratio of 5:3:5. These multiplets can be attributed to 10H, 6H and 10H, respectively. The two multiplets corresponding to 10H each are associated with protons from two sets of equivalent pairs of phenyl groups. The one corresponding to 6H can be assigned to the 6H of three CH₂ groups. The ¹³C NMR spectrum of this ligand exhibits seven distinct signals. The peak at 32.7 ppm corresponds to the C(4) carbon, the one at 51.7 ppm to two equivalent carbons at the C(3) and C(3') positions, the most downfield peak at 196.5 ppm to two equivalent *sp*² carbons (>C=N), and the remaining four peaks ranging from 128-140 ppm to four non-equivalent carbons in each of the four phenyl groups.

Metal complexes: The noncyclic ligand L^{II} forms square planar complexes, [NiL^{II}], [CuL^{II}] and [CoL^{II}], when interacting with Ni(II), Cu(II) and Co(II) salts, respectively. These metal complexes display specific IR bands in their spectra, such as $\nu(\text{C-H})$, $\nu(\text{Ar-H})$, $\nu(\text{CH}_3)$, $\nu(\text{C=N})$, $\nu(\text{C-C})$, $\nu(\text{C-H})\text{Ar}$ and $\nu(\text{M-N})$ (M = Ni, Cu or Co) bands, ranging 2945-2933, 3033-3024, 1359-1355, 1595-1593, 1074-1072, 700-694 and 559-538, respectively. Notably, the absence of acetate bands in the IR spectra of [NiL^{II}] and [CoL^{II}], as well as the absence of perchlorate bands in the IR spectrum of [CuL^{II}], indicates that the acetate and perchlorate anions used for complexation are not present in these complexes. Furthermore, the molar conductivity value of 0 ohm⁻¹ cm² mol⁻¹ for all the complexes in both chloroform and DMSO solvents suggests that these complexes are non-electrolytes, consistent with their square planar structure and the absence of anions. The absence of any OH group bands in the IR spectra indicates that the ligand is deprotonated during complex formation and functions as a dinegative ligand. The electronic spectra of [NiL^{II}] and [CuL^{II}] complexes in DMSO, as well as the [CoL^{II}] complex in chloroform, exhibit *d-d* bands at 563, 549 and 548 nm, respectively, supporting the square planar geometry of these complexes. However, the presence of bands at 731 and 721 nm in the electronic spectra of [NiL^{II}] and [CoL^{II}] complexes in DMSO suggests the formation of octahedral species in DMSO solvent as indicated by the following expression:



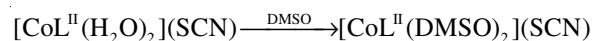
The ¹H NMR spectrum of the [NiL^{II}] complex displays three singlets. Two of these singlets, appearing at 1.54 and 2.00 ppm and accounting for 6H, are attributed to two methyl protons. However, in free ligand, only one singlet was observed for the identical two methyl protons. Another singlet at 5.64

ppm, corresponding to 2H, can be attributed to two CH protons. The appearance of two signals at 3.13 and 3.48 ppm, accounting for 4H, indicates -CH₂-CH₂- protons. In contrast, the free ligand exhibited only one signal for these same protons. Two additional multiplets at 7.32 and 7.76 ppm, each corresponding to 5H, are assigned to protons within two phenyl groups. The spectrum shows no downfield resonance for OH protons, which were present at around 11.50 ppm in the free ligand. It suggests that the OH protons were eliminated through complexation with the metal ion. However, the presence of distinct peaks for the two methyl groups and two -CH₂- groups suggests that complex formation introduced asymmetry into the ligand structure.

In ¹³C NMR spectrum of [NiL^{II}] complex, 9 peaks are observed, as in the free ligand, indicating the presence of 9 non-equivalent carbons. The differences in peak positions in this complex are attributed to the altered electronic environment resulting from the complex formation. Magnetochemical measurements of [NiL^{II}] complex are consistent with a square planar, diamagnetic Ni(II) complex. Conversely, the magnetic moment values of 1.79 B.M. for [CuL^{II}] and 1.75 B.M. for [CoL^{II}] complexes, corresponding to one unpaired electron, align with Cu(II) and Co(II) complexes with *d*⁹ and *d*⁷ configurations, respectively and square planar geometries. Based on the evidence mentioned above, the structures corresponding to [NiL^{II}], [CuL^{II}] and [CoL^{II}] complexes have been assigned as Str. 5, Str. 6, and Str. 7, respectively (Fig. 2).

[CoL^{II}(H₂O)₂](NCS): The reaction between the Co(II) complex [CoL^{II}] of L^{II} and KNCS results in the formation of a hexa-coordinated Co(III) complex, [CoL^{II}(H₂O)₂](SCN). The IR spectrum of this complex displays characteristic bands for $\nu(\text{C-H})$, $\nu(\text{Ar-H})$, $\nu(\text{CH}_3)$, $\nu(\text{C=N})$, $\nu(\text{C-C})$, $\nu(\text{C-H})\text{Ar}$ and $\nu(\text{Co-N})$ in their expected regions. Furthermore, the IR spectrum of this complex exhibits distinctive bands at 2047, 754 and 476 cm⁻¹, which can be attributed to the ionic thiocyanate group [9,10]. Additionally, the complex reveals a band at 3433 cm⁻¹, attributed to νOH , indicating the presence of coordinated water molecules.

The molar conductivity value of 60 ohm⁻¹ cm² mol⁻¹ for this complex in a DMSO solution suggests a 1:1 electrolyte, indicating that the SCN⁻ ion is out of the coordination sphere. In the electronic spectrum of yellow solution of this complex, a *d-d* band at 707 nm is observed, indicating the formation of octahedral species, [CoL^{II}(DMSO)₂](NCS), in DMSO. The appearance of bands at 263 and 261 nm may be attributed to charge transfer transitions.



The magnetic moment measurement of this complex confirms its diamagnetic nature, consistent with expectations for a Co(III) complex featuring a potent ligand with an N₂O₄ donor set and a *d*⁶ electron configuration. Based on the preceding discussion, the structure designated as Str. 8 (Fig. 2) is assigned to the [CoL^{II}(H₂O)₂](NCS) complex.

Antimicrobial studies: Macrocytic complexes involving Ni(II), Cu(II), and Co(III) derived from similar initial components have been documented in previous studies [1,3-6]. These

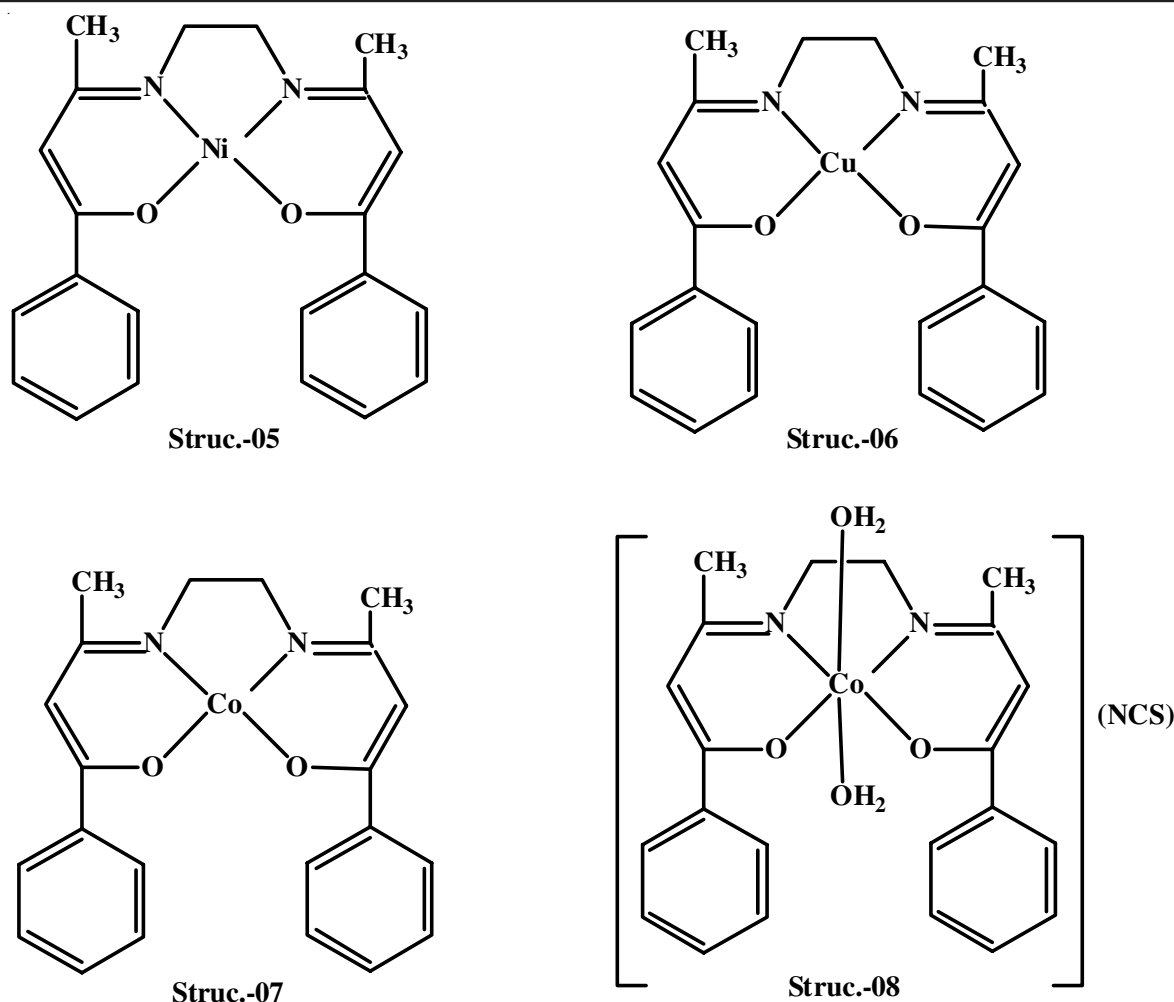


Fig. 2. Structures of the metal complexes of L^{II}

complexes have shown significant antimicrobial activity against various types of bacteria, including Gram-positive and Gram-negative strains and certain harmful fungi. This intriguing finding has motivated the investigation of the antimicrobial properties of the newly synthesized noncyclic ligands and their corresponding metal complexes

Antibacterial efficacy: The effectiveness of both the noncyclic ligands and its complexes involving L^{II} , along with the standard antibiotic Ampicillin, against Gram-positive and Gram-negative bacteria is summarized in Tables 1 and 2, respectively. The results reveal that $[CuL^{II}]$, $[CoL^{II}]$ and $[CoL^{II}(H_2O)_2](SCN)$ (except for their ineffectiveness against Gram-positive bacteria *S. aureus* and Gram-negative bacteria *Vibrio cholerae* and *Pse* species) exhibit potential sensitivity towards three Gram-positive and four Gram-negative bacterial strains. In contrast, L^I , L^{II} , L^{III} (except for their moderate activity against Gram-negative bacteria *S. typhi* and *S. dysenteries*), L^{IV} (except for moderate activity against Gram-positive bacteria *S. aureus*) and $[NiL^{II}]$ do not demonstrate sensitivity against the tested organisms.

Antifungal efficacy: The antifungal effectiveness of the noncyclic ligands and the metal complexes of L^{II} has been assessed against five plant pathogenic fungi. The results of the *in vitro* antifungal investigations of these compounds, along

with the standard antibiotic Nystatin, are provided in Table-3. The $[CoL^{II}]$ displays considerable sensitivity to the mycelial growth of all the tested fungal organisms. However, $[CuL^{II}]$ is not sensitive to plant pathogenic fungi. Furthermore, some tested compounds have shown a stimulatory effect rather than inhibition. Notably most of the ligands were ineffective against these fungi, with exceptions such as L^I , L^{III} and L^{IV} , which demonstrated a significant activity against *F. equiseti* and L^I , which exhibited stimulation against *C. corchori*.

Conclusion

This study observed that three out of the four noncyclic ligands, formed by the condensation of different ketones and amines, underwent decomposition during complexation. In contrast, ligand L^{II} successfully underwent complexation with $Ni(OCOCH_3)_2 \cdot 4H_2O$, $Cu(ClO_4)_2 \cdot 6H_2O$ and $Co(CH_3COO)_2 \cdot 4H_2O$, yielding four coordinated square planar complexes: $[NiL^{II}]$, $[CuL^{II}]$ and $[CoL^{II}]$. Additionally, $[CoL^{II}]$, when exposed to KSCN, produced a Co(III) complex, $[CoL^{II}(H_2O)_2](NCS)$. It is worth noting that while Co is known to form Co(III) octahedral complexes with macrocyclic ligands, it can also form both square planar Co(II) and octahedral Co(III) complexes with noncyclic analogs. All the complexes, except $[CoL^{II}(H_2O)_2]$ -

TABLE-1
ANTIBACTERIAL EFFECTS OF THE COMPOUNDS ON GRAM-POSITIVE BACTERIA

Ligand and complexes (100 µg dw disc)	Zone of inhibition (mm) after 24 and 48 h								
	<i>B. cereus</i>		<i>B. subtilis</i>		<i>S. aureus</i>		<i>B. magaterium</i>		
	24 h	48 h	24 h	48 h	24 h	48 h	24 h	48 h	
L ^I	0	0	0	0	0	0	0	0	0
L ^{II}	0	0	0	0	0	0	0	0	0
L ^{III}	0	0	0	0	0	0	0	0	0
L ^{IV}	0	0	0	0	7	7	0	0	0
[NiL ^{II}]	0	0	0	0	0	0	0	0	0
[CuL ^{II}]	14	14	14	15	0	0	13	14	14
[CoL ^{II}]	10	10	12	13	0	0	8	8	8
[CoL ^{II}](NCS)	15	15	15	16	0	0	15	15	15
Ampicillin	16	–	25	–	24	–	19	–	–

TABLE-2
ANTIBACTERIAL EFFECTS OF THE COMPOUNDS ON GRAM-NEGATIVE BACTERIA

Ligand and complexes (100 µg dw disc)	Zone of inhibition (mm) after 24 and 48 h											
	<i>E. coli</i>		<i>V. cholera</i>		<i>S. typhi</i>		<i>S. paratyphi</i>		<i>Pse. species</i>		<i>S. dysenterie</i>	
	24 h	48 h	24 h	48 h	24 h	48 h	24 h	48 h	24 h	48 h	24 h	48 h
L ^I	0	0	0	0	0	0	0	0	0	0	0	0
L ^{II}	0	0	0	0	0	0	0	0	0	0	0	0
L ^{III}	0	0	0	0	6	6	0	0	0	0	7	7
L ^{IV}	0	0	0	0	0	0	0	0	0	0	0	0
[NiL ^{II}]	0	0	0	0	0	0	0	0	0	0	0	0
[CuL ^{II}]	14	15	0	0	13	14	12	12	0	0	15	15
[CoL ^{II}]	12	12	0	0	12	12	17	17	0	0	10	10
[CoL ^{II}](NCS)	15	17	0	0	17	17	20	20	0	0	13	14
Ampicillin	30	–	32	–	25	–	28	–	35	–	35	–

TABLE-3
ANTIFUNGAL ACTIVITIES OF THE COMPOUNDS

Ligand and complexes	% Inhibition of mycelial growth				
	<i>M. phaseolina</i>	<i>C. lunata</i>	<i>F. equiseti</i>	<i>C. corchori</i>	<i>A. alternate</i>
L ^I	0	0	23	+11	0
L ^{II}	0	0	0	0	0
L ^{III}	0	0	21	0	0
L ^{IV}	0	0	15	0	0
[CuL ^{II}]	0	0	0	0	0
[NiL ^{II}]	0	0	7	+22	0
[CoL ^{II}]	22	21	30	22	22
[CoL ^{II}](NCS)	0	0	15	+11	0
Nystatin	76	70	45	41	51

(NCS), were found to be non-electrolytes, in line with the expected square planar geometry, with no anions outside the coordination sphere. The tested bacteria generally displayed minimal response to the synthesized ligands. However, three complexes, namely [CuL^{II}], [CoL^{II}] and [CoL^{II}], exhibited moderate resistance against the tested bacterial strains. On the other hand, regarding antifungal efficacy studies, it was observed that the noncyclic ligands and their complexes were less effective in inhibiting fungal growth compared to macrocyclic ligands and their complexes.

ACKNOWLEDGEMENTS

Partial funding for this research was provided through grants from the Environmental Radioactivity Research Network

Center (ERAN: I-23-17) at Fukushima University, Japan and the Japan Society for the Promotion of Science (JSPS) under Grants-in-Aid for Scientific Research (21K12287).

CONFLICT OF INTEREST

The authors declare that there is no conflict of interests regarding the publication of this article.

REFERENCES

- R. Amin, S. Rabi, L. Barua, M.N. Uddin, M.I. Morshed, I.M.M. Rahman and T.G. Roy, *Asian J. Chem.*, **35**, 447 (2023); <https://doi.org/10.14233/ajchem.2023.26929>
- A. Chakraborty, S. Rabi, L. Dey, D. Palit, B.K. Dey, E.R.T. Tiekink and T.G. Roy, *Heliyon*, **8**, e09678 (2022); <https://doi.org/10.1016/j.heliyon.2022.e09678>

3. M.A. Sayed, S. Rabi, P. Paul, L. Dey, B.K. Dey, Z.A. Begum, I.M.M. Rahman and T.G. Roy, *J. Incl. Phenom. Macrocycl. Chem.*, **102**, 251 (2022); <https://doi.org/10.1007/s10847-021-01110-5>
4. L. Dey, S. Rabi, D. Palit, S.K.S. Hazari, Z.A. Begum, I.M.M. Rahman and T.G. Roy, *J. Mol. Struct.*, **1240**, 130579 (2021); <https://doi.org/10.1016/j.molstruc.2021.130579>
5. L. Dey, S. Rabi, S.K.S. Hazari, T.G. Roy, A. Buchholz and W. Plass, *Inorg. Chim. Acta*, **517**, 120172 (2021); <https://doi.org/10.1016/j.ica.2020.120172>
6. R.E. Benson, T.G. Roy, B.K. Dey, K.K. Barua and E.R.T. Tiekink, *Acta Crystallogr. Sect. E Struct. Rep. Online*, **62**, o1971 (2006); <https://doi.org/10.1107/S1600536806013614>
7. M. Tasumi, T. Urano and M. Nakata, *J. Mol. Struct.*, **146**, 383 (1986); [https://doi.org/10.1016/0022-2860\(86\)80306-4](https://doi.org/10.1016/0022-2860(86)80306-4)
8. R.J. Bose and M.D. Peters, *Can. J. Chem.*, **49**, 1766 (1971); <https://doi.org/10.1139/v71-288>
9. M.E. Farago and J.M. James, *Inorg. Chem.*, **4**, 1706 (1965); <https://doi.org/10.1021/ic50034a007>
10. A. Sabatini and I. Bertini, *Inorg. Chem.*, **4**, 959 (1965); <https://doi.org/10.1021/ic50029a007>